"Physics of Auroral Phenomena", Proc. XLV Annual Seminar, Apatity, pp. 78-81, 2022

Polar Geophysical Institute

DOI: 10.51981/2588-0039.2022.45.018

OBSERVATIONAL PROPERTIES OF CORONAL MASS EJECTIONS (CMES) ASSOCIATED WITH THE SOFT X-RAYS AND GEO-EFFECTIVENESS DURING SOLAR CYCLES 23 AND 24

Priyank Srivastava, A.K. Singh

Physics Department, University of Lucknow, Lucknow-226007, India

Abstract

The principal agents responsible for spatial weather changes and associated phenomena are coronal mass ejections (CMEs). The geo-effectiveness of CMEs has a large impact on terrestrial climate. CME detection and computation remain tough because to the variety of forms and the complexity of the progression of time. As a result, in order to assess the variable's viability, we examined the regular changes of the total, northern, and southern components of sunspot counts recorded between 1996 and 2020, as well as the solar activity trend for solar cycles 23 and 24. We discovered that solar activity was lower in solar cycle 24 than it was in cycle 23. Based on these results, we concluded that, while the number of CMEs detected in the 24th solar cycle (16680) was more than in the 23rd solar cycle (13640), solar activity fell in cycle 24, which might be connected with the lower geo-effectiveness of CMEs seen during cycle 24. The strength of the flare in optical or X-rays does not indicate the intensity of the ensuing geomagnetic activity. C and M class flares have been linked to severe storms (Dst < -100 nT). The Pearson's correlation coefficient between the initial speed of CMEs and geomagnetic activity was determined to be 0.66, which is moderate and negative. This link shows that the initial speed of halo CMEs is related to geo-effectiveness prediction. Thus, we determined that the solar cycle 24 was weakly active in comparison to the solar cycle 23, and that there was a declining pattern in solar activity based on the number of sunspots and the examination of the observational characteristics of CMEs and their occurrence, as well as geo-effectiveness.

1. Introduction

Coronal Mass Ejections are a significant solar violent event that hurls enormous amounts of magnetic flux and plasma out of the solar atmosphere, with the potential to have repercussions on the heliosphere, interplanetary space, and Earth's atmosphere (*Webb and Howard*, 2012; *Lamy et al.*, 2019). These are the most striking events associated with the dynamic Sun and the primary aspect of space weather that further affect the Sun-Earth system (*Singh et al.*, 2010, 2014). CMEs provide pathways for the separation from the Sun of an enormous amount of magnetic flux and helical flux, which forms the basis for another solar cycle. CMEs play an important role in the solar dynamo by ejected magnetic helicity (*Webb and Howard*, 2012).

Knowledge of CMEs associated with solar surface activities, as well as with the Earth, has significant importance since the method of initiating CMEs would raise understanding of the physical link between the solar magnetic field and its activity (*Singh et al.*, 2010). *Subramanian and Dere* (2001) analysed coronal mass ejections detected between January 1996 and May 1998 and concluded that approximately 41% of CMEs were related with active regions (ARs) and occurred without prominence eruptions, 44% of CMEs observed were associated with eruptions with active region prominence, while 15% of CMEs observed were associated with quiescent prominence. In their study of CMEs in the years 1997 to 2001. There's some evidence that solar dynamic processes owing to horizontal surface mobility of magnetic flux persist well into solar cycle decline, as *Jang et al.* (2016) hypothesized. In recent years, remote sensing devices, in-situ data, and certain models have been utilized to explain the source mechanism, propagation, and absence of shock associated with the CMEs (*Nieves-Chinchilla et al.*, 2020; *Giacalone et al.*, 2020).

Section 1 includes a short introduction to the characteristics of coronal mass ejections. Information about data sources is provided in section 2. Section 3 discussed the solar activity and the rate of CMEs. The link between Coronal Mass Ejections and geomagnetic storms, as well as some of SC 23's major storms, are discussed in section 4. Results and discussion are described in section 5 and finally, conclusions are presented in section 6.

2. Data Sources

The data used in the present study for statistical analysis are obtained from the catalogue of SOHO's website (https://cdaw.gsfc.nasa.gov/CME_list/catalog_description.htm) as the LASCO is observing CMEs continuously since January 1996 (since the start of solar cycle 23). We have analyzed all the ejection events (CMEs) observed during solar cycles 23 and 24. For studying the variations in the sunspot numbers, we have evaluated sunspot number data from the World Data Centre SILSO from January 1996 to June 2020. The total number of observations was 8887, and

we have also derived the daily total, north and south sunspot numbers. The Dst indices were collected from the World Data Center geomagnetic activity web page (http://swdcwww.kugi.kyoto-u.ac.jp).

3. Solar Activity and CME rate

The only confrontational route for analyzing the prolonged evolution of the solar cycle is the time series of sunspot numbers and is widely used in various fields, especially in Solar Physics. It offers crucial information on multiple observational properties as their higher and lower numbers are closely related to solar activity (*Singh and Bhargawa*, 2017, 2019). Figure 1 represents the differences in the daily average SSN and the daily north/south SSN in the years 1996-2020 (solar cycles 23 & 24). Figure 1 demonstrates that the solar cycle 23 sunspot number was greater than the solar cycle 24 count, indicating that solar activity was stronger during the solar cycle 23 compared to the sunspot count during the solar cycle 24. In addition, the graph shows a time series plot of the north/south sunspot counts observed during solar cycles 23 and 24. In solar cycle 23, the mean value of sunspots in the north was ~36.97 and ~41.84 in the south, whereas in solar cycle 24, the mean value of sunspots in the north was ~25.11 and ~23.03 in the south. These differences in the north and the south sunspot numbers are known as N-S asymmetry concerning the equator and this asymmetry is always present in the solar cycles during the rising or declining phases. Studies of the N-S asymmetry and its link to solar activity have been conducted by a variety of researchers (*Verma*, 1993; *Ballester et al.*, 2005). Based on the mean values observed in the present study, we can conclude that solar cycle 23 was south dominant and solar cycle 24 was north dominant. The mean of total sunspot numbers in solar cycles 23 and 24 were ~78.82 and ~48.15. This difference in the sunspot numbers, clearly suggests that solar cycle 24 is magnetically weaker than solar cycle 23.

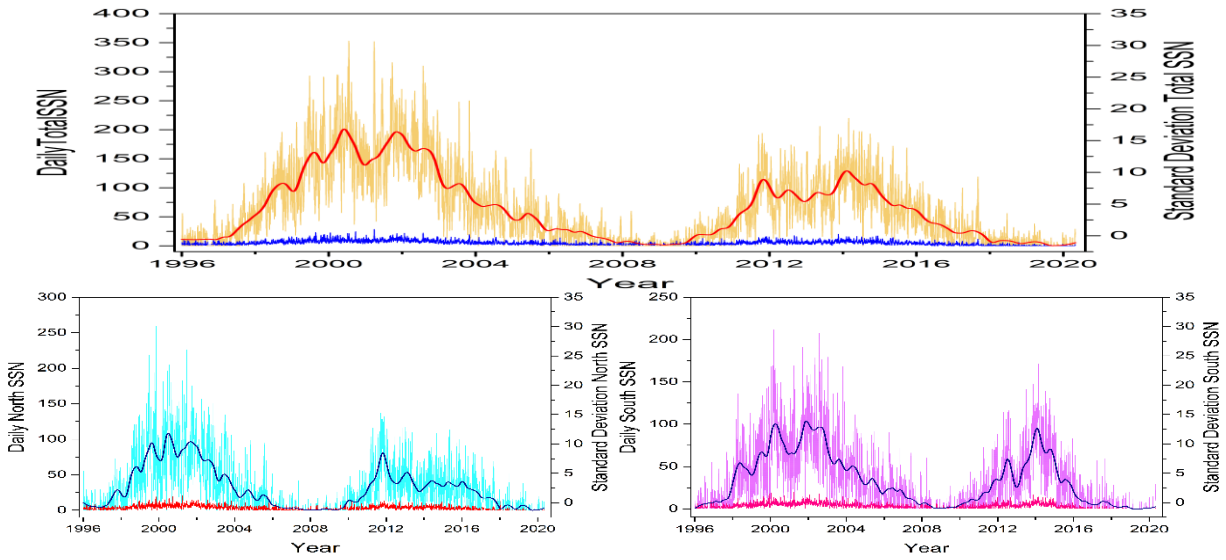

Figure 1. Time series plot for daily total, north and south sunspot numbers observed during solar cycles 23 (1996-2008) and 24 (2008-2020).

4. Coronal mass ejections (CMEs) and geomagnetic storms

The geomagnetic storm is one of the immediate repercussions of CMEs entering the magnetosphere of the Earth. The ecliptic component (Bz) of the IMF is the key link between a geomagnetic storm and a CME (*Gopalswamy et al.*, 2009). The cause of geomagnetic storms is the re-joining of the CME field and the magnetic field of the Earth when Bz is pointing south (*Gopalswamy*, 2008). The Bz component in the quiescent solar wind is insignificant, but CMEs contain Bz due to their flux rope structure. The compressed sheath field between the flux rope and the shock can also contain Bz since fast CMEs generate shocks (*Manchester et al.*, 2005). This means that Bz can arise from the flux rope and sheath. The Dst index (in nT) is a measure of the strength of geomagnetic storms and is calculated from the horizontal component of the Earth's magnetic field recorded at several equatorial sites (*Sabaka et al.*, 2004). Most major storms are triggered by CMEs and have Dst ≤ −100 nT (*Zhang et al.*, 2007). Table 1 shows the list of CMEs associated geo-magnetic storms.

5. Results and Discussion

One of the early indicators of a weak solar cycle 24 was the significantly reduced number of large geomagnetic storms (Dst ≤ −100 nT) (*Kilpua et al.*, 2014). Figure 2 depicts a time series plot of the Dst index, revealing that the frequency and amplitude of storms in cycle 24 are the lowest in the space age (cycles 19 to 24). Storms with Dst < −200 nT occurred in every cycle since 1957, except for cycle 24, when storms never exceeded 140 nT. Several historical storms

may be identified in the figure 2, including recent ones on 14 March 1989 with Dst = -589 nT and 20 November 2003 with Dst = -422 nT.

Table 1. List of geo effective coronal mass ejections with associated geomagnetic storms (Dst ≤ -300).

High speed CMEs	**Linear Speed**	**Travel time (hrs)**	**Associated X-ray events**	**Region**	**Dst (nT)**	**E > 10 MeV**
CME of July 14, 2000	1674 km/s	27.71	X5/3b, M3/1n	9077 (N18W09)	-301	24000 pfu
CME of March 28, 2001	1600 km/s	60.03	M1/Sf, M1/Sn, M4/Sf, M1/1f	9393 (N13E00)	-387	1100 pfu
CME of October 28, 2003	2000 km/s	18.68	X17/4b	486 (S17E04)	140	29500 pfu
CME of October 29, 2003	2029 km/s	19.48	X10, M3	486 (S17W09)	-30	3300 pfu
CME of November 18, 2003	1824 km/s	47.21	M3/2n, M9	501 (N03E09)	55	98 pfu
CME of November 4, 2004	1055 km/s	66.95	M5/sn, M2/1n, M4/1f	696 (N09E06)	-374	72 pfu

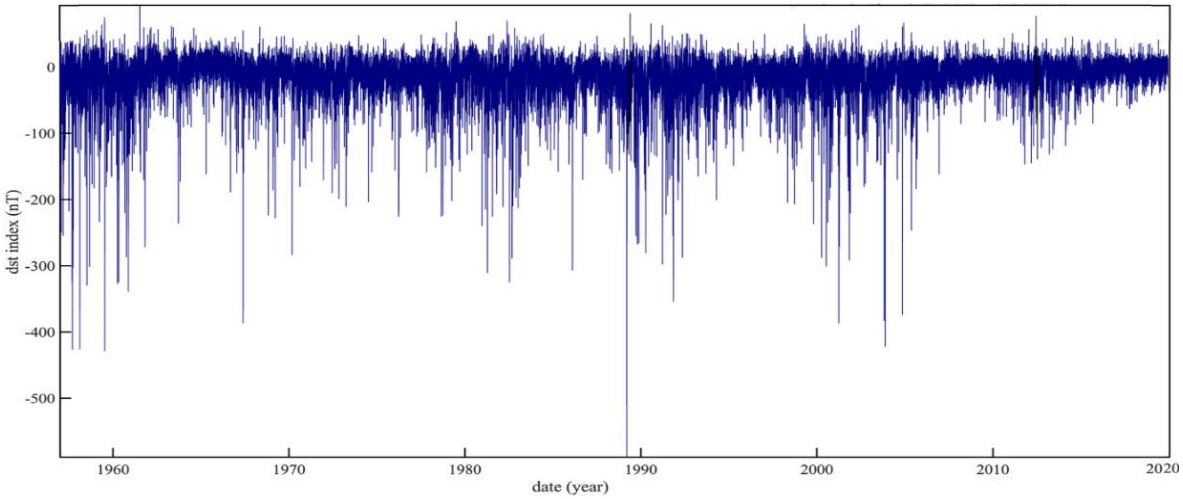

Figure 2. The Dst index as a function of time from 1957 to 2020.

For the period 1996 to 2020, we analyzed all 91 geo-effectiveness of CMEs that generated severe geomagnetic storms (DST index less than -100 nT). According to recent studies by LASCO, CMEs display certain different features independent of their direction of motion. For all geoeffective CMEs recorded between 1996 and 2020, the starting speeds vary from 500 to 2500 km/h in the FOV of LASCO-C2. Pearson's coefficient of 0.66 was shown to be negatively correlated with geomagnetic activity and therefore, the initial speed of the CME and the storm's DST strength are moderately correlated (Figure 3*a*).

Figure 3 illustrates that the severe geomagnetic storms are connected with solar flares of class X and M that originated from the central-northern area, and these flares came from old active regions. X17/4b and X10/2b were the two most powerful flares of solar cycle 23. They were both produced by Region 486 located in southern part near the equator. M class flares were found to be concentrated in the central northern region of the sun near the equator, whereas C class flares erupted from the western and eastern limbs (Figure 3*b*).

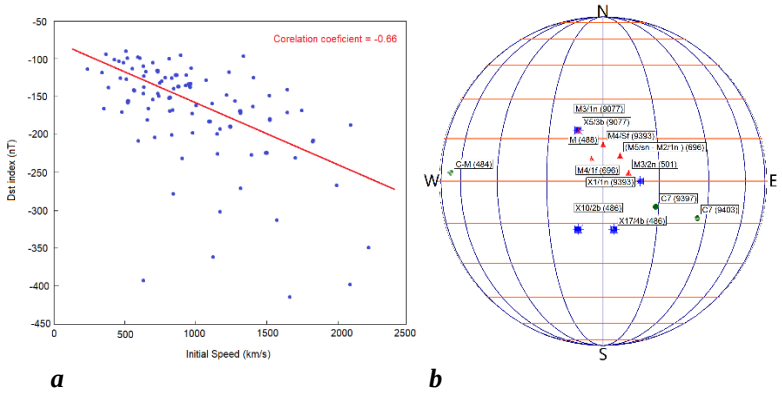

a ***b***

Figure 3. Location of intense solar flares (X, M, C class used in case study of extreme geomagnetic storm) as a function of solar longitude (in degrees) and active regions associated with the flares.

6. Conclusion

As part of the present work, we have studied several observational characteristics of CMEs during solar cycles 23 and 24 from 1996 to 2020. We have collated various aspects of CMEs about the overall solar activity represented by the total and hemispherical sunspot numbers. The following are some of the most important conclusions from this statistical analysis:

- We depicted differences in the sunspot numbers in the north and south hemispheres in the solar cycles 23 and 24 which prominently shows the existence of N-S asymmetry.
- Geomagnetic activity during solar cycle 24 was very low as compared to its three precursors.
- The strength of the flare in optical or X-ray images does not accurately predict the intensity of the geomagnetic activity that would occur. However, even C and M class flares can be accompanied by severe storms (Dst > -100 nT).
- The initial speed of CMEs and geomagnetic activity was found to have a moderate and negative Pearson's correlation coefficient of 0.66. This correlation suggests that the prediction of geo-effectiveness is associated with the initial speed of halo CMEs.
- In our case study of geomagnetic storms, we discovered that the majority of the intense solar flares (mostly X and M class) causing the extreme geomagnetic events originate from the former active regions in the central north hemispherical region near the equator, while low M and C class are near the eastern and western limbs.

References

Ballester J.L., Oliver R., Carbonell M. 2005, A&A, 431, L5-L8
Giacalone J., Mitchell D.G., Allen R.C., et al. 2020, Astrophys. J., 246, 29
Gopalswamy N. 2008, J. Atmos. Sol. Terr. Physics, 70(17), 2078-2100
Gopalswamy N., Dal Lago A., Yashiro S., and Akiyama S. 2009, Central European Astrophysical Bulletin, 33, 115
Jang M., Woods T.N., Hong S., Choe G.S. 2016, ApJ, 833, L11
Kilpua E.K.J., Luhmann J.G., Jian L.K., Russell C.T., and Li Y. 2014, J. Atmos. Sol. Terr. Physics, 107, 12-19
Lamy P.L., Floyd O., Boclet B. et al. 2019, Space Sci. Rev., 215, 39
Manchester W.B., Gombosi T.I., De Zeeuw D.L. 2005, The Astrophysical Journal, 622(2), 1225
Nieves-Chinchilla T., Szabo A., Korreck K.E., et al. 2020, Astrophys. J., 246, 63
Sabaka T.J., Olsen N., Purucker M.E. 2004, Geophysical Journal International, 159(2), 521-547
Singh A.K., Siingh D., Singh R.P. 2010, Surveys in Geophysics, 31, 581-638
Singh, A.K., Tonk, A., Singh, R. 2014, Indian J. Physics, 88, 2711-2716
Singh A.K., Bhargawa A. 2017, Astrophys. Space Sci., 362, 199
Singh A.K., Bhargawa A. 2019, Astrophys. Space Sci., 364, 12
Subramanian P., Dere K.P. 2001, Astrophys. J., 561, 372
Verma V.K. 1993, Astrophys. J., 403, 797-800
Webb D.F., Howard T.A. 2012, Sol. Phys., 9, 3
Zhang J., Richardson I.G., Webb D.F., et al. 2007, Journal of Geophysical Research: Space Physics, 112(A10), A10102